

# Cross section for the $^{103}\text{Rh}(n,n')^{103}\text{Rh}^m$ reaction in the energy range 5.7–12 MeV

M. M. H. Miah,\* B. Strohmaier, and H. Vonach

*Institut für Radiumforschung und Kernphysik der Universität Wien, Boltzmannngasse 3, A-1090 Wien, Austria*

W. Mannhart and D. Schmidt

*Physikalisch-Technische Bundesanstalt, Bundesallee 100, D-38116 Braunschweig, Germany*

(Received 22 November 1995)

The  $^{103}\text{Rh}(n,n')^{103}\text{Rh}^m$  cross section was measured by the activation method in the neutron energy range 5.7–12 MeV with an uncertainty of  $\approx 5\%$ . Monoenergetic neutrons produced by the  $D(d,n)^3\text{He}$  reaction were used to irradiate metallic Rh samples at  $0^\circ$  relative to the deuteron beam. The  $K$  x rays from  $^{103}\text{Rh}^m$  were measured with a calibrated Si detector, and the neutron fluence was determined by means of a  $^{238}\text{U}$  fission chamber. The measured cross sections resolve the discrepancies in previous data and agree with the results of recent statistical model calculations of the fast-neutron cross sections of rhodium. [S0556-2813(96)02207-8]

PACS number(s): 25.40.Fq, 24.10.Eq, 24.60.Dr, 27.60.+j

## I. INTRODUCTION

Cross sections for the formation of isomeric levels in fast neutron reactions can provide a very sensitive test for nuclear reaction models, if there is sufficient knowledge about the relevant model parameters, especially the level schemes of the respective nucleus and the optical-model parameters. The  $^{103}\text{Rh}(n,n')^{103}\text{Rh}^m$  reaction is a very favorable case in this respect. The level scheme including information on spin, parity, and branching ratios is known up to about 1.3 MeV [1], and careful recent measurements of total and differential elastic neutron cross sections [2] have very much reduced the uncertainties of the optical-model parameters. In addition, the  $^{103}\text{Rh}(n,n')^{103}\text{Rh}^m$  reaction is of considerable interest in neutron metrology. Because of its low threshold of 40 keV it can be used for fast neutron fluence determinations in reactor neutron dosimetry.

Up to 6 MeV, two activation measurements of the  $^{103}\text{Rh}(n,n')^{103}\text{Rh}^m$  cross sections were carried out previously [3,4], which are in reasonable agreement with both each other and with indirect determinations of cross sections from  $(n,n'\gamma)$  data [5]. Between 6 and 13 MeV, however, there is only a single activation measurement [4] which is partly contradictory as it shows rather large discrepancies between the results obtained using two different neutron source reactions, namely  $D(d,n)^3\text{He}$  ( $DD$ ) and  $T(p,n)^3\text{He}$  ( $TP$ ).

For these reasons, new measurements of the  $^{103}\text{Rh}(n,n')^{103}\text{Rh}^m$  cross section were performed in the energy range 5.7–12 MeV using the  $DD$  reaction as a neutron source. No measurements above 12 MeV were performed as the correction for the breakup neutrons produced in the deuteron-deuteron interaction rises very steeply with deuteron energy and prevents accurate cross-section measurements above about 12 MeV.

The experiment is described in Sec. II; in Sec. III the results are presented, discussed, and compared with existing

data and statistical model calculations.

A preliminary report on the experiment was presented at the International Conference on Nuclear Data for Science and Technology, Gatlinburg 1994 [6].

## II. EXPERIMENTAL METHOD

Neutrons with energies between 5.69 and 12 MeV were produced via the  $DD$  reaction. Deuterons extracted from the PTB compact cyclotron CV-28 interacted with a gas target, 3 cm long and operated at a pressure of 0.2 MPa [7]. The neutron energy at  $0^\circ$  (relative to the deuteron beam) was determined by time-of-flight measurements using an NE-213 liquid scintillation detector at 12 m distance. Metallic rhodium samples, 0.125 mm thick and 10 mm in diameter, were attached to the front of a low-mass fission chamber (Fig. 1) and were also irradiated at  $0^\circ$  at a distance of 60 mm from the gas target. The mean neutron energy averaged over the sample was found to be  $\pm 20$  keV in the mentioned time-of-flight measurements and the target-sample geometry. The neutron energy resolution (FWHM), determined from the deuteron energy loss in the target gas and the target sample

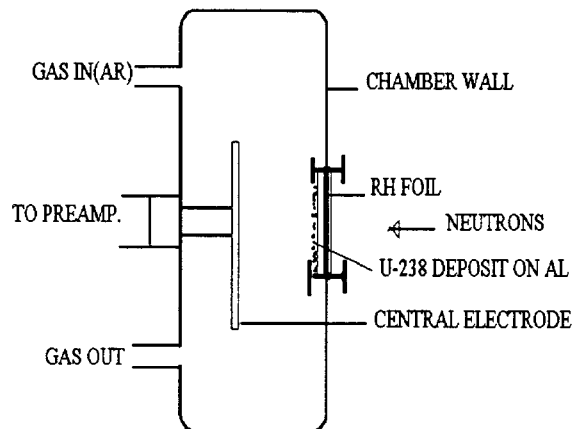


FIG. 1. Arrangement of sample and  $^{238}\text{U}$  deposit in the fission chamber.

\*On leave for Ph.D. studies from the Department of Physics, University of Chittagong, Chittagong, Bangladesh.

geometry, varied from 0.210 to 0.108 MeV for  $E_n = 5.7\text{--}12$  MeV.

An enriched (99.8%)  $^{238}\text{U}$  fission deposit with a mass of  $102.10 \pm 0.52 \mu\text{g}$  [8] (see Fig. 1) was used to determine the neutron fluence applying the ENDF/B-VI evaluation [9] for the  $^{238}\text{U}$  fission cross section. The ionization chamber was operated with pure Ar gas. The pulse-height spectrum of the fission fragments was clearly separated by a flat region from  $\alpha$  particles from neutron-induced reactions and  $^{238}\text{U}$  decay. The observed fission rate was corrected by horizontal extrapolation to zero pulse height and by a self-absorption correction derived in previous measurements using this fission deposit [10,11]. Irradiations of 1–3 h, depending on the  $^{238}\text{U}$  fission cross section, were chosen in order to obtain a sufficient number of fission pulses. At each neutron energy a gas-out measurement was performed in order to correct for the contributions of the neutrons produced in window and backing of the gas target.

The  $K$  shell x rays of  $^{103}\text{Rh}^m$  (summed area of the  $K_\alpha$  and  $K_\beta$  peaks) were measured by means of a Si(Li) x-ray detector (area  $200 \text{ mm}^2$ , thickness of Be window 0.05 mm). Its efficiency was calibrated using x-ray point sources of  $^{109}\text{Cd}$  and  $^{93}\text{Nb}^m$  whose activity was accurately known. The variations of the efficiency for an extended source and for self-absorption in the samples were taken into account very carefully. For the self-absorption correction, the mass attenuation coefficient  $\mu/\rho$  was determined experimentally from the count rates of a Rh sample with and without transmission through an inactive foil. The experimental value ( $14.34 \text{ cm}^2/\text{g}$ ) of  $\mu/\rho$  is in good agreement with the theoretically calculated value [12]. Using this experimental value, the self-absorption factors for the corresponding samples were calculated to be  $\{1 - \exp[-(\mu/\rho)(\rho d)]\}/[(\mu/\rho)(\rho d)]$ , where  $\rho$  is the density and  $d$  the thickness of the Rh sample. This expression is valid for a small solid angle in which the photons can pass nearly perpendicularly through the absorbing foil.

At the beginning of the experiment, a separate irradiation was made to check for interfering reactions of different half-lives by observing the decay curve. No indication of activities other than the 56.114-min activity of  $^{103}\text{Rh}^m$  was found in the investigated time range from 10 to 80 min after the end of irradiation. Accordingly, the measurements were started as soon as possible ( $\approx 14\text{--}26$  min after the end of irradiation). The counts of the low-energy x rays from the irradiated samples were measured by placing the sample very close to the window of the detector, whereas the calibration measurements were performed at a distance of 18.55 mm in order to have a sufficiently small solid angle allowing an accurate correction for self-absorption. The counting period for each run was 3600 sec. The count rates of the sample in the measurement position were converted to the calibrated position using a conversion factor determined experimentally. This factor was determined from the ratio of count rates obtained with the same irradiated samples in calibration and measurement position, resulting in a value of  $5.732 \pm 0.49\%$ . The background was measured using a nonirradiated Rh foil of the same dimension as the irradiated foil in measurement position. A value of  $0.0766 \pm 1.83\%$  [13] was used for the total  $K$  x-ray emission probability in the  $^{103}\text{Rh}^m$  decay.

Both the measured x-ray intensity and the fission fragment counts were corrected for the effect of neutrons scattered elastically or inelastically in the samples or the adjacent parts of the fission chamber, for neutrons produced in the window and backing of the gas target, and for breakup neutrons produced in the target gas itself by  $D(d,np)D$  processes.

The corrections for scattered neutrons were calculated by Monte Carlo methods [14]. In order to correct for neutrons produced in the target window and backing, both x-ray and fission counts from the gas-out measurements were subtracted from the corresponding gas-in measurements after normalization to the same total deuteron charge.

The correction for the effect of breakup neutrons turned out to be the most important one. Although it is negligible up to 8 MeV, it increases very steeply above this energy, and at  $E_n = 12$  MeV, about 65% of the observed  $^{103}\text{Rh}^m$  activity and 33% of the fission rate are due to breakup neutrons. A special iterative procedure was, therefore, developed to determine this correction as accurately as possible. The intensity of the breakup neutrons relative to the monoenergetic  $DD$  neutrons and their spectra were measured accurately (to about  $\pm 5\%$ ) at PTB for the angular range from  $0^\circ$  to  $15^\circ$  and our range of neutron energies [7]. As a first approximation, the contributions of the breakup neutrons to both fission rate and activation were calculated by folding the results of Ref. [7] with the cross sections for the  $^{238}\text{U}(n,f)$  and the  $^{103}\text{Rh}(n,n')^{103}\text{Rh}^m$  reactions using ENDF/B-VI values for the former reaction and the results of the evaluation by Strohmaier *et al.* [15] for the latter. This procedure is sufficient for the fission rates; concerning the activation we must consider that our recent measurement improves our knowledge of the  $^{103}\text{Rh}(n,n')^{103}\text{Rh}^m$  reaction compared with Ref. [15]. A revised evaluation of the  $^{103}\text{Rh}(n,n')^{103}\text{Rh}^m$  cross section was, therefore, performed including the preliminary results of this experiment with the corrections described above. Then, as a second approximation, the breakup correction to the  $^{103}\text{Rh}^m$  production was recalculated using the excitation function evaluated in this way. As the cross-section changes due to this step turned out to be small ( $< 3\%$ ), the result of this second iteration was adopted as our final result. The uncertainty of the breakup corrections was calculated from the covariances resulting from this revised evaluation run and the uncertainties given in Ref. [7].

### III. RESULTS AND DISCUSSION

The values of the cross sections for each mean neutron energy and the neutron energy resolution are given in Table I. The principal sources of uncertainty are shown in Table II. The uncertainties are effective ( $1\sigma$ ) standard deviations and were obtained by quadratic addition of all uncertainty components. The uncertainties increase considerably toward the highest neutron energies due to the increasing breakup correction.

In Fig. 2 our results are compared with the previous measurements of Paulsen and Liskien [3] and Santry and Butler [4]. In these experiments, values of 0.0843 and 0.0697, respectively, for the  $K$  x-ray emission probability resulted as by-products. The data were, therefore, renormalized to the value of 0.0766 adopted by us, using the factors 1.10 (Ref.

TABLE I. Measured  $^{103}\text{Rh}(n,n')^{103}\text{Rh}^m$  cross sections.

Average neutron energy (MeV)	Resolution (FWHM) (MeV)	Cross section (mb)	Uncertainty (mb)
$12.003 \pm 0.020$	0.108	565	45
$11.424 \pm 0.020$	0.108	721	49
$11.039 \pm 0.020$	0.110	771	47
$10.579 \pm 0.020$	0.112	938	48
$9.915 \pm 0.020$	0.116	1195	50
$9.550 \pm 0.020$	0.120	1228	48
$8.965 \pm 0.020$	0.124	1221	44
$8.550 \pm 0.020$	0.130	1293	48
$7.979 \pm 0.020$	0.136	1247	44
$7.575 \pm 0.020$	0.144	1203	43
$6.932 \pm 0.020$	0.160	1321	46
$6.525 \pm 0.020$	0.172	1312	49
$6.039 \pm 0.020$	0.190	1296	46
$5.689 \pm 0.020$	0.210	1314	58

[3]) and 0.91 (Ref. [4]). In addition, the values of Ref. [4] measured with the aid of the  $DD$  reaction [and, below  $E_n=0.55$  MeV, the  $^7\text{Li}(p,n)^7\text{Be}$  reaction] and derived from measurements using the  $TP$  reaction are displayed by different symbols. As can be seen from the figure, there is excellent agreement between our values, the results of Ref. [3], and those data of Ref. [4] which were measured by means of

the  $DD$  reaction, whereas the data points of Santry and Butler [4] measured by means of  $TP$  neutrons are considerably smaller and probably suffer from some undetected systematic error.

Both our results and the  $DD$  results of Ref. [4] indicate that the  $^{103}\text{Rh}(n,n')^{103}\text{Rh}^m$  cross section is approximately constant in the energy region from 6 to 10 MeV as had been

TABLE II. The principal sources and the resulting magnitude of uncertainty in the measured cross sections.

Source of uncertainty	Resulting uncertainty (%)
For the activity measurement of $^{103}\text{Rh}^m$ :	
$K$ x-ray counting (statistics of net count rates in gas-in run)	0.63–0.89
Subtraction of activities from gas-out run	0.30–1.30
Transfer factor from measurement position to calibrated position	0.49
Efficiency of the Si(Li) x-ray detector including the average over the sample area	1.80
Self-absorption of the x rays in the sample	1.08–1.13
Activity due to elastically and inelastically scattered neutrons	0.12–0.22
Activity correction due to breakup neutrons	0.05–6.78
Half-life of $^{103}\text{Rh}$	0.036
Emission probability of $K$ x rays	1.83
Mass of Rh foil	Negligible
For the neutron fluence measurement:	
Fission fragment counting statistics (gas-in run)	1.02–1.51
Subtraction of fission fragments from gas-out run	0.30–1.84
Extrapolation correction for fission fragments	0.35–1.81
Self-absorption of $^{238}\text{U}$ deposit	0.14–0.25
Reference cross section of $^{238}\text{U}$	0.93–1.47
Mass calibration of $^{238}\text{U}$	0.59
Fluence transformation from monitor to sample level	0.07
Fission fragments due to secondary neutrons	Negligible
Fission fragments due to breakup neutrons	0.01–1.73
Neutron attenuation between sample and monitor	0.06
Correction for flux fluctuation	Negligible

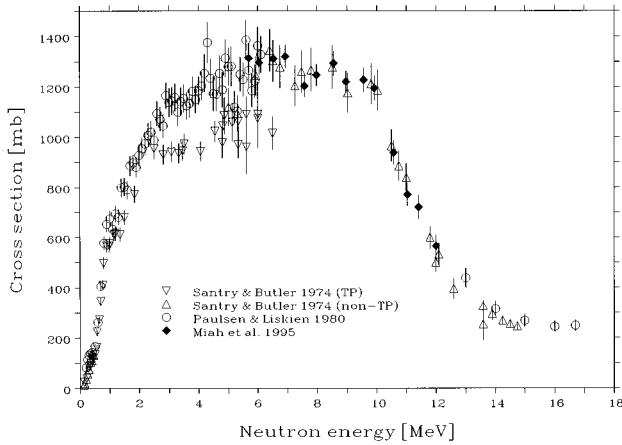


FIG. 2. Cross sections for the  $^{103}\text{Rh}(n,n')^{103}\text{Rh}^m$  reaction resulting from the present experiment compared with those from the measurements by Paulsen and Liskien [3] and by Santry and Butler [4]. Regarding the data of Ref. [4], the display distinguishes between  $T(p,n)^3\text{He}$  and other neutron-source reactions by the use of different symbols. Apart from the 10 data points with  $E_n < 0.5$  MeV measured with the  $^7\text{Li}(p,n)^7\text{Be}$  source reaction, “non-TP” is synonymous to  $DD$ .

expected theoretically [15,16]. In Fig. 3, our results are compared with a number of calculations based on the statistical model of nuclear reactions. The determination of the model parameters and the options chosen for the calculations with the STAPRE code are described in detail in Ref. [16]. The solid line in Fig. 3 corresponds to the result which was considered the best fit in an attempt to optimize the overall reproduction of the experimental excitation functions for the reactions  $^{103}\text{Rh}(n,n')^{103}\text{Rh}^m$ ,  $^{103}\text{Rh}(n,2n)^{102m,g,(m+g)}\text{Rh}$ ,  $^{103}\text{Rh}(n,3n)^{101m,(m+g)}\text{Rh}$ ,  $^{103}\text{Rh}(n,p)^{103}\text{Ru}$ , and  $^{103}\text{Rh}(n,\alpha)^{100}\text{Tc}$  from the respective thresholds up to 30 MeV incident neutron energy. As is obvious from the figure, there is agreement between this calculation and our data, as

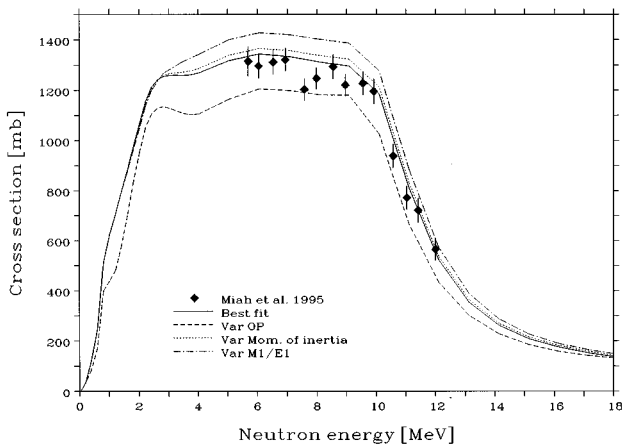


FIG. 3. Cross sections for the  $^{103}\text{Rh}(n,n')^{103}\text{Rh}^m$  reaction resulting from the present experiment compared with the results of nuclear model calculations. Solid line, parameters as in Ref. [16]; dashed line, neutron optical potential of Ref. [17] used (instead of that of Ref. [2]); dotted line, moment of inertia equal to rigid-body value (instead of 75% of rigid-body value); dash-dotted line, ratio of strengths of  $M1$  to  $E1$  radiation at the neutron-binding energy increased by a factor of 6 with respect to Ref. [16].

the given error bars refer to  $1\sigma$  uncertainty. In order to assess the meaning of this result, it is necessary to consider the effect of parameter variations (within their estimated uncertainties) on the calculated cross sections. As the emission of charged particles does not play a significant role in this mass range, the reactions that share the absorption cross section in the incident energy range considered for the present experiment are  $(n,n')^{m,g}$  and  $(n,2n)^{m,g}$ . The proportion of the  $(n,n')$  and  $(n,2n)$  cross sections is mainly determined by the position of the  $(n,2n)$  threshold, with a minor influence of level densities, the choice of the preequilibrium matrix element, and the parameters of  $\gamma$  decay of  $^{103}\text{Rh}$  near the neutron-binding energy. The main tools for controlling the magnitude of the  $^{103}\text{Rh}(n,n')^{103}\text{Rh}^m$  cross section are, therefore, the neutron optical potential defining the transmission coefficients for formation of the compound nucleus and its decay into neutron channels, further the moment of inertia relevant to the angular-momentum distribution of the population of  $^{103}\text{Rh}$  resulting from neutron emission from  $^{104}\text{Rh}$ , and, finally, the relative strengths of  $E1$  and  $M1$  radiation in the  $\gamma$  decay of the continuum states of  $^{103}\text{Rh}$ . To demonstrate the influence of these quantities, Fig. 3 also comprises the excitation functions for the  $^{103}\text{Rh}(n,n')^{103}\text{Rh}^m$  reaction calculated with neutron transmission coefficients derived from the global optical potential given by Igarasi [17] instead of that of Smith and Guenther [2], with moments of inertia equaling the rigid-body values (rather than 75% of these as in Ref. [16]), and with a ratio of  $M1$  to  $E1$  strength at the neutron-binding energy in  $^{103}\text{Rh}$  increased by a factor of 6 with respect to the value assumed in Ref. [16]. These parameter variations were each done leaving the other two at the best-fit values. A variation of the  $E2$  strength in magnitude (increase by a factor of 3), but not in shape (Weisskopf model), was also tested and found to have negligible effect on the  $^{103}\text{Rh}(n,n')^{103}\text{Rh}^m$  excitation function.

As regards these parameter variations, the case of the optical potential is a special one. The optical potential of Smith and Guenther [2], derived from accurate measurements of angular distributions of elastically scattered neutrons, of angle-integrated cross sections for the population of groups of levels in  $^{103}\text{Rh}$ , and of total cross sections, yields certainly a more realistic description of neutron absorption and emission in various decay channels than any other global optical potential such as that of Igarasi [17]. This is also confirmed by the much better description of the  $(n,2n)$  and  $(n,3n)$  excitation functions in their onsets right above the thresholds by the Smith-Guenther potential and its ability of accurately describing the inelastic scattering of neutrons on Rh in the low-energy range of discrete levels. In contrast to the other parameter variations which are our best estimates of the cross-section uncertainties because our knowledge of these parameters is restricted, the uncertainty of the cross sections due to the deficiencies inherent in the potential of Smith and Guenther can now be safely assumed to be smaller than the difference between our “best-fit” and “Igarasi potential” calculations.

Keeping this in mind, we may conclude the following from Fig. 3.

In the energy region below the  $(n,2n)$  threshold ( $E_n = 9.32$  MeV), the cross section is sensitive to only three of the parameters considered, namely to optical potential,

moment of inertia and ratio of  $M1$  to  $E1$  strength. Since the influence of the moment of inertia is considerably smaller than that of the remaining two parameters, this finding amounts to an ambiguity with respect to optical potential and  $M1/E1$  ratio, i.e., the combination of Igarasi potential and increased  $M1/E1$  may give an equally good or—judging just by the quality of fit to the  $^{103}\text{Rh}(n,n')^{103}\text{Rh}^m$  excitation function—improved fit. However, due to the virtues of the Smith-Guenther potential discussed above, we still prefer the use of the latter together with the smaller value of  $M1/E1$ , without attributing much significance to the parameters of the  $M1$  giant resonance.

In the neutron energy range above the  $(n,2n)$  threshold, the cross section also becomes somewhat sensitive to other parameters such as total  $\gamma$ -ray strength or preequilibrium matrix element; no specific information on any of these parameters can be obtained from the comparison with our data.

What is most important, however, due to the low sensitivity of the  $^{103}\text{Rh}(n,n')^{103}\text{Rh}^m$  cross section to all param-

eters our data provide a rather sensitive test of the statistical model of nuclear reactions itself. As is evident from Fig. 3, all admissible parameter variations produce deviations from our best fit by about 10%. Thus, the agreement between our data and our theoretical best fit implies that any additional model deficiencies will not result in larger variations either, and that, within these limits, uncertainties of similar cross-section calculations may be estimated safely from the uncertainties of the parameters entering into the calculations.

#### ACKNOWLEDGMENTS

We are grateful to Dr. K. Debertin and the technical staff of the PTB, Braunschweig, for permitting the use of the laboratory facilities for the measurement of x-ray activities and for the careful operation of the cyclotron. Thanks are also due to Dr. M. Wagner for her contributions towards the experiment in its early stages.

- 
- [1] M. J. Martin and J. K. Tuli, Nucl. Data Sheets **68**, 311 (1993).
- [2] A. B. Smith and P. Guenther, "Fast-neutron interaction with the fission product  $^{103}\text{Rh}$ ," Argonne National Laboratory Report ANL/NDM-130, 1993.
- [3] A. Paulsen and H. Liskien, Nucl. Sci. Eng. **76**, 331 (1980).
- [4] D. C. Santry and J. P. Butler, Can. J. Phys. **52**, 1421 (1974).
- [5] E. Barnard and D. Reitmann, Nucl. Phys. **A303**, 27 (1978).
- [6] M. M. H. Miah, H. Vonach, W. Mannhart, and D. Schmidt, in *Proceedings of the International Conference on Nuclear Data for Science and Technology*, Gatlinburg, TN, 1994, edited by J. K. Dickens (American Nuclear Society, LaGrange Park, IL, 1994), p. 278.
- [7] S. Cabral, G. Börker, H. Klein, and W. Mannhart, Nucl. Sci. Eng. **106**, 308 (1990).
- [8] M. Wagner, private communication.
- [9] ENDF/B-VI, Evaluated Nuclear Data File, as received from the IAEA, Nuclear Data Section, Vienna (1994).
- [10] M. Wagner, G. Winkler, and H. Vonach, Ann. Nucl. Energy **15**, 363 (1988).
- [11] M. Wagner, G. Winkler, H. Vonach, and H. Liskien, in *Proceedings of the International Conference on Nuclear Data for Science and Technology*, Mito, Japan, 1988, edited by S. Igarasi (Saikon, Tokyo, 1988).
- [12] E. Storm and H. Israel, Nucl. Data Tables **7**, 598 (1970).
- [13] U. Schötzig, Appl. Radiat. Isot. **45**, 641 (1994).
- [14] A. Pavlik, private communication.
- [15] B. Strohmaier, S. Tagesen, and H. Vonach, Phys. Data **13-2**, 87 (1980).
- [16] B. Strohmaier, Ann. Nucl. Energy **22**, 687 (1995).
- [17] S. Igarasi, in *Proceedings of the 4th Conference on Nuclear Cross sections and Technology*, Washington, D.C., 1975, edited by R. A. Schrack and C. D. Bowman (National Bureau of Standards, Washington, D.C., 1975).